need their values.

With $n\mu \equiv M_S$, we have

$$H' = -4\pi M_S\left(\frac{e}{mc}\right)xp_y - \left(\frac{e\mu}{mc}\right)p_y \sum_{\vec{G}\neq 0} C_{\vec{G}}^{x} e^{i\vec{G}\cdot\vec{x}} + \cdots. \tag{5}$$

The oscillatory part of H' is invariant under a lattice translation and may therefore be added to the unperturbed Bloch Hamiltonian to give eigenfunctions of the Bloch form. The usual spin-orbit interaction (not considered in H') is oscillatory and is disposed of in the same way. The remainder $-4\pi M_S(e/mc)xp_y$ of H' is equal to the $\vec{A}\cdot\vec{p}$ term in the kinetic energy

$$\frac{1}{2m}\left(\vec{p}-\frac{e}{c}\vec{A}\right)^2 = \frac{1}{2m}p^2 - \frac{e}{mc}\vec{A}\cdot\vec{p} + \frac{e^2}{2mc^2}A^2, \tag{6}$$

provided

$$\vec{A} = (0, 4\pi M_S x, 0). \tag{7}$$

This is just the vector potential of a magnetic field $H_0^z = 4\pi M_S$.

The oscillatory contribution to $\vec{A}$ is of the order $\mu_B/a^2 \sim 10^{-4}$ cgs; the order of magnitude of the smooth contribution is $4\pi M_S R_C \sim 10^{-1}$ cgs, where the cyclotron radius R_C has been taken as 10^{-5} cm in a 50-kG applied field. Thus it appears that we may neglect in A^2 the terms arising from the square of the oscillatory component of $\vec{A}$ and also terms in the product of the smooth and oscillatory components. In any event the oscillatory parts of A^2 are to be treated as part of the Bloch Hamiltonian. Our estimate $A_{\mathrm{osc}} \sim 10^{-4}$ cgs may underestimate an s-state component; we might rather take A_{osc} as of the order of a Compton wavelength times a hyperfine field, or $10^{-10}\times 10^{7} \approx 10^{-3}$ cgs, which is still small compared to $4\pi M_S R_C$.

Our result is that the contribution of the magnetization to the effective internal magnetic field acting on the momentum of a conduction electron is $4\pi M_S$, very closely, provided that the interaction process is elastic.[4] The value is essentially independent of the details of the conduction electron eigenstates.

I am indebted to Dr. A. V. Gold for a stimulating talk and for a preprint of his paper.

*Assisted by the National Science Foundation.

[1]J. R. Anderson and A. V. Gold, Phys. Rev. Letters 10, 227 (1963). J. R. Anderson, A. V. Gold, and P. T. Panousis, Bull. Am. Phys. Soc. 8, 258 (1963).

[2]G. H. Wannier, Phys. Rev. 72, 304 (1947); see also the papers by Swann and by Webster referred to here.

[3]H. A. Kramers, Grundlagen der Quantentheorie (Akademische Verlagsgesellschaft, Leipzig, Germany, 1938), p. 239.

[4]Electron-electron inelastic collisions typically are rather infrequent because of effective screening of the Coulomb interaction. It is possible, however, that d-d or s-d collisions (enhanced by a high density of states of d electrons at the Fermi level) may be sufficiently frequent in some ferromagnetic metals to make it impossible to observe a de Haas–van Alphen effect except at very low temperatures.

LYMAN ALPHA PRODUCTION IN PROTON-RARE GAS COLLISIONS*

Donavon Pretzer, Bert Van Zyl, and Ronald Geballe
Department of Physics, University of Washington, Seattle, Washington
(Received 11 March 1963)

Nonresonant charge-exchange cross sections for proton-rare gas collisions have been measured by several investigators.[1] Almost without exception the cross sections versus energy exhibit a single, rather broad maximum. We have measured the emission of Lyman alpha radiation from collisions of 1- to 25-keV protons with rare gas atoms. These measurements show two prominent maxima in the Lyman alpha-producing reactions for $H^+ + Ne$, $H^+ + Ar$, and $H^+ + Kr$. The cross section for $H^+ + Xe$ has a peak at 10 keV and gives an indication of another at very low proton energy. The $H^+ + He$ cross section does not show two distinct peaks in the energy range of our apparatus, but there does seem to be a shoulder on the high-energy side of the maximum. Figs. 1 and 2 are a presentation of the measured cross section versus incident proton energy in the lab system for the five rare gases. The argon curve is the average of 5 runs with two different gas samples. The helium and krypton curves are the average of 4 runs each; the xenon, 3 runs; and the neon, 2 runs. All curves are reproducible to within ±5%.

The basic apparatus and detection scheme are described elsewhere.[2] Modifications include the

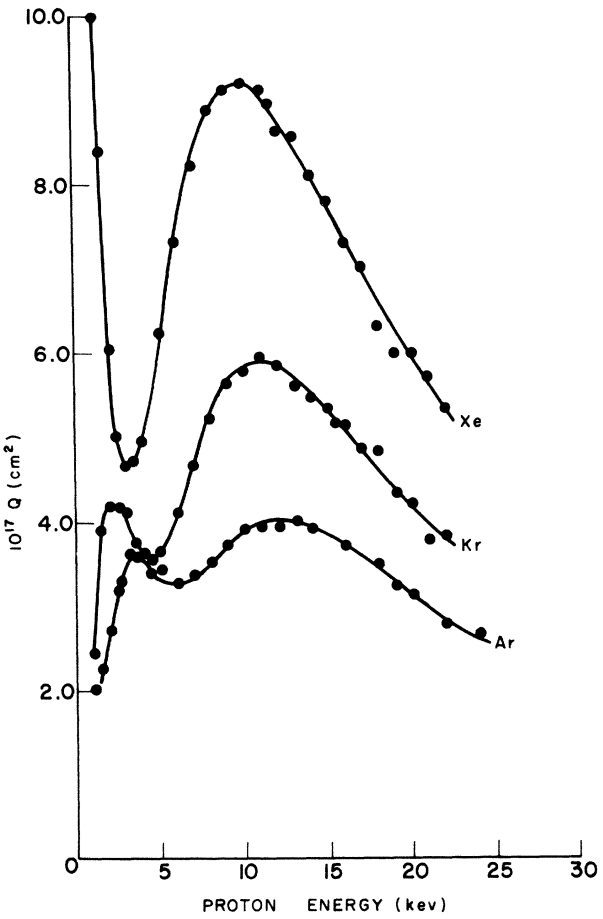

FIG. 1. Cross section for Lyman alpha production from H^+ on Ar, Kr, and Xe.

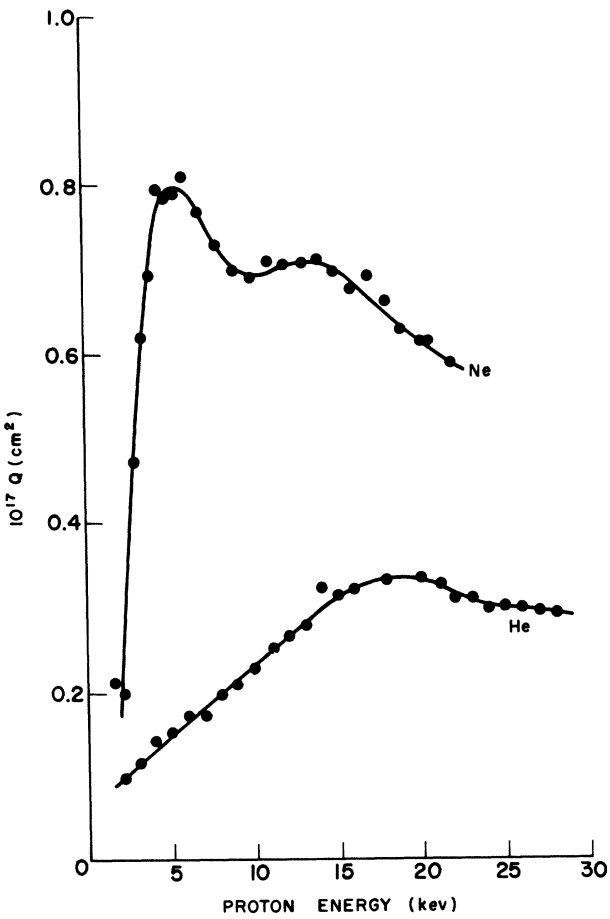

FIG. 2. Cross section for Lyman alpha production from H^+ on He and Ne.

extension of the proton energy range and the use of a pressure-monitored target gas cell. Pressures in the cell ranged from about 3×10^{-4} mm-Hg for helium to 1.5×10^{-5} for xenon. The detector is a helium-iodine photon counter, described by Brackmann, Fite, and Hagen,[3] used in conjunction with an oxygen gas filter. Although the interpretation of the results obtained with this detector could be ambiguous, a variety of tests on the data have convinced the authors that the radiation observed is primarily Lyman alpha. All signals were found to be linear with pressure and proton current. Absolute values of the cross sections are within ±45%. The oxygen window at 1215 Å is quite narrow, and since the source of radiation is an extended one, a correction for Doppler shift is necessary even for right-angle viewing. Preliminary measurements of this effect show that the main features of the cross-section curve would not be changed appreciably by correction.

The authors are extending the work in an effort to explain the occurrence of the dual peaks found in these reactions. We comment briefly on three papers that may be relevant to the final analysis.

The results presented here might be related to the total charge-transfer cross sections of reference 1. For example, in the case of $H^+ + Xe$ our 10-keV peak lies at about the same energy as the small deviation exhibited by their experimental points and ignored by Stedeford in drawing a smooth curve. Their points for the pair $H^+ + Kr$ exhibit a similar deviation of smaller magnitude.

The work of Everhart et al.,[4] in which scattering at 5° was studied, shows oscillations of the scattered neutral beam intensity when plotted against proton energy. Our low-energy maxima in Ne, Ar, and Kr occur at about the same energies as the initial peaks observed by them. This relationship suggests that charge transfer to an

excited state of hydrogen must under certain conditions result in appreciable scattering.

Bates[5] has suggested the possibility of dual peaks in charge-transfer cross sections arising from pseudocrossing of potential energy surfaces.

*Work supported in part by the U. S. Army Research Office (Durham) and the U. S. Office of Naval Research.

[1]J. B. H. Stedeford and J. B. Hasted, Proc. Roy. Soc. (London) A227, 466 (1955); R. H. Hughes, J. L. Philpot, J. G. Dodd, and S. Lin, Technical Report, Contract AF19(604)-4966, University of Arkansas, September, 1962 (unpublished).

[2]G. H. Dunn, R. Geballe, and D. Pretzer, Phys. Rev. 128, 2200 (1962).

[3]R. T. Brackmann, W. L. Fite, and K. E. Hagen, Rev. Sci. Instr. 29, 125 (1958).

[4]F. P. Ziemba, G. J. Lockwood, G. H. Morgan, and E. Everhart, Phys. Rev. 118, 1552 (1960).

[5]D. R. Bates, Proc. Roy. Soc. A257, 22 (1960).

LASER BEAM INDUCED ELECTRON EMISSION

David Lichtman and J. F. Ready
Honeywell Research Center, Hopkins, Minnesota
(Received 8 March 1963)

Sharp pulses of electron emission have been observed emanating from the target used in studying beam-surface interaction in vacuum. As part of a program studying the effects of beam-induced gas desorption in ultrahigh vacuum, experiments were performed using focused laser beams on "dag"-coated metal targets. The "dag" used is colloidal carbon in isopropyl alcohol and organic (glycol) binder. While monitoring the gas desorption processes, effects were observed which indicated the emission of an electron current from the target during application of the laser beam. The magnitude of the current was considerable, and its appearance in time relative to the laser pulse was extremely rapid. Experiments were performed to determine quantitatively the magnitude of the electron pulse as well as its shape. The experimental system is shown in Fig. 1.

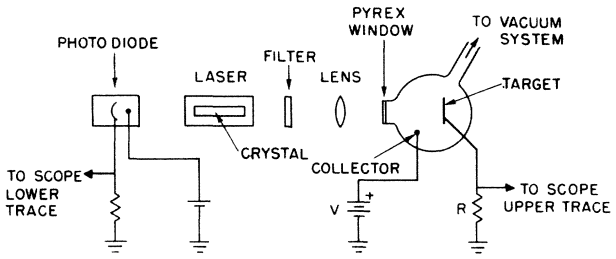

FIG. 1. Configuration of experimental setup. Laser output is obtained from both ends of the laser crystal providing simultaneous signals for photodetector and target bombardment. Measurements were also taken with the oscilloscope probe connected to the collector. The vacuum system is ion-pumped.

In the preliminary experiments, a ruby laser produced a total output pulse of approximately one joule over a total pulse length of approximately 800 microseconds. The output of the laser was focused with a simple lens onto the target, providing a target spot size of approximately 10^{-3} cm^2. Suitable filters were used to insure that only the 1.78-eV photons were being transmitted to the target. A typical laser output and current pulse output are shown in Fig. 2. The very rapid fall-off of current pulses after the first 150 μsec of laser output is not well un-

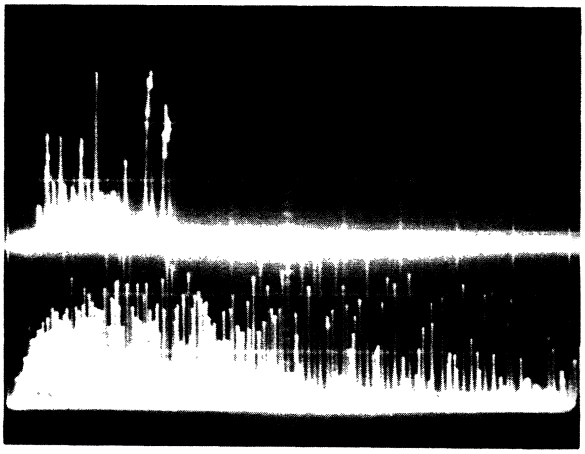

FIG. 2. Scope traces showing electron emission due to absorption of ruby laser beam by carbon target. Lower trace is output of ruby laser. Time scale is 50 μsec/cm. Upper trace shows electron emission pulses. Amplitude scale corresponds to 20 mA/cm. Collector is positive with respect to the target.